Biosensors and Bioelectronics 126 (2019) 657–663

Contents lists available at ScienceDirect

Biosensors and Bioelectronics

journal homepage: www.elsevier.com/locate/bios

A label-free electrochemical biosensor for microRNAs detection based on DNA nanomaterial by coupling with Y-shaped DNA structure and non-linear hybridization chain reaction

Lin Zhou[a], Yang Wang[a], Cheng Yang[a], Huan Xu[a], Jie Luo[a], Wenqing Zhang[a], Xiaoqi Tang[a], Sha Yang[a], Weiling Fu[a], Kai Chang[c,*], Ming Chen[a,b,d,**]

[a] Department of Clinical Laboratory Medicine, Southwest Hospital, Third Military Medical University, 30 Gaotanyan, Shapingba District, Chongqing 400038, China
[b] College of Pharmacy and Laboratory Medicine, Third Military Medical University, 30 Gaotanyan, Shapingba District, Chongqing 400038, China
[c] Department of Clinical Laboratory Medicine, Institute of Surgery Research, Daping Hospital, Third Military Medical University, 10 Changjiangzhilu, Yuzhong District, Chongqing 400042, China
[d] State Key Laboratory of Trauma, Burn and Combined Injury, Third Military Medical University, 30 Gaotanyan, Shapingba District, Chongqing 400038, China

ARTICLE INFO

Keywords:
MicroRNA
DNA nanomaterial
Y-shaped DNA
Non-linear hybridization chain reaction
Biosensor

ABSTRACT

DNA nanomaterials have been widely used in bioassays due to their promising properties for sensitive and specific detection of biomolecules. Herein, a label-free electrochemical method was developed for quantitative detection of microRNAs by integrating Y-shaped DNA (Y-DNA) structures with non-linear hybridization chain reaction (non-linear HCR). The Y-DNA structures consisting of three sequences (Y1, Y2 and Y3) serve as stable and specific probes for recognizing target miRNAs. In the presence of target miRNA, competitive hybridization occurs between miRNA and Y-DNA, resulting in the release of Y3 and the disintegration of the Y-DNA structure. The triggers, which were blocked by Y3 previously, were exposed and initiated the non-linear HCR. Remarkable electrochemical signal changes were produced after the isothermal amplification reaction. Therefore, the proposed biosensor achieved sensitive detection of microRNAs (miRNAs). Under optimal conditions, the limit of detection (LOD) was reduced to 0.3334 fM and linear range was from 1 fM to 10 pM. The special design of Y-DNA helped the biosensor obtain the ability to distinguish between single base mutations. What's more, this biosensor was capable of detecting miRNAs in clinical serum samples. We hope that this developed biosensor would provide a potential application for DNA nanomaterials in the field of microRNAs detection and inspire more interests in the development of DNA nanomaterial biosensors.

1. Introduction

MicroRNAs (miRNAs) are short non-coding RNA molecules, which play significant roles in a variety of biological processes, especially in cancer developments (Hausser and Zavolan, 2014; Yates et al., 2013). Since miRNAs are involved in the development and progression of diseases, numerous studies have attempted to use them for clinical assays (Papadaki et al., 2018; Franklin et al., 2018). For instance, China Food and Drug Administration (CFDA) has approved a miRNAs kit for diagnosing early liver cancer in 2017 (Zhou et al., 2011). Thus, the sensitive and specific detection of miRNAs is considered to be a meaningful way to come true early cancer diagnosis (Tian et al., 2015). Currently, traditional methods, mainly including northern blotting, microarray analysis and RT-PCR, are hardly applied to clinic bioassays (Urbanek et al., 2015; Flowers et al., 2013). These methods have the disadvantages of complicated operations, high prices and unstable results. Besides, direct determination of miRNAs is still a realistic challenge due to their small size, instability and low serum abundance (G. Liu et al., 2018). In recent years, numerous biosensing techniques have been implemented to make sensitive detection of miRNAs because of their unique detection and analysis principles, such as electrochemistry, fluorescent, electrochemiluminescence (ECL), surface plasmon resonance (SPR) and surface-enhanced Raman scattering (SERS) (Azzouzi et al., 2017; Lu et al., 2017, 2018; Hu et al., 2017; He et al., 2017). The electrochemical biosensor has received greater attention in clinical diagnosis due to its easy controllability, high sensitivity and low cost (Su

* Corresponding author.
** Corresponding author at: Department of Clinical Laboratory Medicine, Southwest Hospital, Third Military Medical University, 30 Gaotanyan, Shapingba District, Chongqing 400038, China.
E-mail addresses: changkai0203@163.com (K. Chang), chming1971@126.com (M. Chen).

https://doi.org/10.1016/j.bios.2018.11.028
Received 11 October 2018; Received in revised form 16 November 2018; Accepted 18 November 2018
Available online 20 November 2018
0956-5663/

et al., 2016; Xu et al., 2018). Therefore, the biomolecular recognition and signal amplification based on electrochemical platform to achieve miRNAs detection still need to be considered.

Recently, nanomaterials have emerged as versatile tools for biological detection, such as metal-based nanomaterials, polymer-based nanomaterials and carbon-based nanomaterials (Nehra and Pal Singh, 2015). DNA as a neglected biomaterial can be applied in this filed, since it has high operability and selectivity (Ye et al., 2018; Zhang et al., 2017). Over the last decades, numerous nucleic acid nanostructures have been applied to biological detection, including DNA dendrimers, DNA tetrahedron, DNA gels, and so on (Brown et al., 2017; L. Zhou et al., 2017; X. Zhou et al., 2017). Y-shaped DNA (Y-DNA), as a stable nanostructure with high selectivity, provides an effective method for precisely measuring target molecules (Li et al., 2018). Y-DNA is composed of three oligonucleotides which partially hybridize to each other. Some previous biosensors used this feature to achieve DNA determinations in which one DNA stand was fixed on the surface, another DNA stand and target DNA were introduced to form a specific structure (Wang et al., 2015; Li et al., 2004). For example, Wang's group have achieved DNA detection by using a target sequence and several assistant sequences to construct a Y-shaped junction scaffold-mediated modular (Liu et al., 2015). However, such methods did not fully exploit the advantages of their high selectivity since hybridization could also be achieved even with a little bit flaw. In addition, the lack of signal amplification methods made it hard to achieve ultra-sensitive detection.

Numbers of signal amplification strategies have been developed, including rolling circle amplification (RCA), catalytic hairpin assembly (CHA), strand displacement amplification (SDA) and hybridization chain reaction (HCR) (Peng et al., 2018a; C. Liu et al., 2018; Miao et al., 2018; Peng et al., 2018b). HCR is consisted of a trigger sequence and two partially complementary hairpin probes. Once triggered, the two hairpin probes could continuous hybridize autonomously (Niu et al., 2010; Bi et al., 2017). Lately, non-linear hybridization chain reaction (HCR) has evolved the conventional HCR from linear probes hybridization to complicated branched probes hybridization (Xuan and Hsing, 2014). Compared to HCR, this reaction is composed of more complex components, including a trigger sequence, two double-stranded substrates with bridge loops in the middle and two auxiliary sequences (Chang et al., 2016). Thus, non-linear HCR could achieve higher amplification ratios and molecular weights (Ding et al., 2017). To combine non-linear HCR and Y-DNA nanostructures, the terminals of Y-DNA were designed as triggers which could initiate the amplification reaction. As a result, the novel biosensing method could achieve high sensitive and selective detection of biological molecules.

Herein, we aimed at designing a label-free DNA nanostructure electrochemical biosensor for the detection of miRNA-25, which was reported to be a potential molecular biomarker for non-small cell lung cancer and heart failure (Xu et al., 2014; Wahlquist et al., 2014). In this strategy, Y-DNA was employed as a specific probe because of its good stability and selectivity. Considering of the instability and low abundance of miRNAs, a competitive binding method was employed in the proposed biosensor to recognize miRNA-25. When miRNA-25 was introduced, it could hybridize to one of the sequences constituting the Y-DNA, resulting in the decomposition of Y-DNA. The protected triggers were exposed and could initiate non-linear HCR consequentially. According to the above design, DNA nanomaterial can achieve successful miRNAs detection in human serums without the assistants of other materials, enzymes and labels. Hence, this strategy provides a novel label-free DNA nanomaterial electrochemical biosensor for detecting miRNAs, which might contribute to the early cancer diagnosis and clinical analysis.

2. Materials and methods

2.1. Reagents

DNA sequences were manufactured by TaKaRa Biotechnology Company (Dalian, China) and purified by high-performance liquid chromatography (Table S1). Tris (2-carbosyethyl) phosphine hydrochloride (TCEP) and 6-mercapto-1-hexanol (MCH) were obtained from Sigma-Aldrich (St Louis, MO, USA). Super GelRed nuclear staining was procured from US Everbright Inc. (Suzhou, China). TBE buffer was obtained from Solarbio Life Sciences (Beijing, China). Piranha solution was a mixture of 30% hydrogen peroxide and 98% sulfuric acid in a ratio of 1:3. Phosphate buffered saline (PBS) buffer was purchased from Hyclone Labotatories (Utah, USA). Hybridization buffer (40 mM Tris-base, 20 mM acetic acid, 2 mM EDTA, 12.5 mM magnesium acetate), competitive buffer (1 mM Tris-HCl, 25 mM NaCl, 1 mM EDTA) and [Fe $(CN)_6]^{3-/4-}$ solution (5 mM [Fe $(CN)_6]^{3-/4-}$, 0.1 M KCl) were prepared by the laboratory. All chemical reagents used were of analytical reagent grade and without further purification. All solutions were dissolved in ultrapure water from Millipore water purification system (> 18MΩcm, Millipore, USA).

2.2. Apparatus

All electrochemical measurements were carried out with a CHI 760E electrochemical work station (Shanghai Chenhua, China) using a traditional three-electrode system that consisted of a platinum wire electrode as the counter electrode, a saturated calomel electrode (SCE) as the reference electrode and a gold electrode (GE) as the working electrode. Polyacrylamide gel electrophoresis (PAGE) was conducted by a Bio-Red imaging system (California, USA). Polymerase chain reaction (PCR) machine was purchased from Applied Biosystems Inc. (California, USA) and dry bath incubator was obtained from Tiangen Biotech Co. Led (Beijing, China).

2.3. Preparation of Y-DNA and substrates

Y-DNA was prepared by mixing equimolar amounts of three single-stranded DNA (ssDNA), including two longer ssDNAs and a shorter one. The two longer sequences have domains that hybridize to the shorter one respectively. However, one of the domain did not completely bind to the corresponding part, so that target miRNA could replace this moiety and dismantle the Y-DNA nanostructure. These ssDNAs were dissolved in hybridization buffer at a final concentration of 10 μM for each sequence and annealed to form desired Y-shaped DNA using the following process: annealed at 95 °C for 2 min, cooled to 65 °C and incubated for 5 min, then dropped to 60 °C for 2 min and cooled to 20 °C at a rate of 1 °C per minute. The final products were stored at 4 °C.

In addition, the two double-stranded substrates of non-linear HCR were also needed to be prepared in advance. The double-stranded substrate 1 (S1) was formed by mixing S1a and S1b in hybridization buffer. The mixture was heated to 95 °C for 5 min and slowly cooled to 4 °C, then allowed to stand at room temperature for 20 min to form a specific double-stranded substrate. The substrate 2 (S2) was obtained in the same way as described above. The final products were also stored at 4 °C for further use.

2.4. Electrochemical detection procedure

The gold electrodes were polished to mirror faces with alumina slurry (0.3 and 0.05 μm) in sequence, followed by ultrasonication in ethanol and water for 1 min. Then electrodes were rinsed with ultrapure water and dried with nitrogen. Afterwards, the gold electrodes were washed with fresh piranha solution for 10 min to eliminate the adsorption of organic substances, followed by washing with pure water and drying with nitrogen. Next, the gold electrodes were activated in a

0.5 M H_2SO_4 solution by scanning the potential between 0 V and 1.6 V until a stable gold oxide status was obtained. So far, the gold electrodes were ready for bioassays. The prepared Y-DNA probes were diluted to wanted concentration and disposed by 1 mM TCEP to reduce disulfide bonds. Then, 3 μL of activated Y-DNA probes were dropped on the surface of gold electrodes and incubated at 37 ℃ overnight. The uncovered sites of modified electrodes were blocked by dropping MCH (1 μM) on the surface at 4 ℃ for 1 h. After washing with water, the electrodes were immersed in the competitive buffer containing a certain concentration of target miRNA and incubated at 35 ℃ for 120 min to dismantle the Y-DNA nanostructures and expose the trigger ends. Non-bonded residues and new by-products were washed away by PBS carefully. Later, the modified electrodes were immersed in 300 μL of hybridization buffer containing non-linear HCR components, including early prepared substrate 1, 2 and helper 1, 2. After incubation at 39 ℃ for 3 h, the electrodes were washed with PBS to remove unfixed sequences. All concentrations, reaction times and temperatures were optimized to achieve high efficiency. Electrochemical measurements included cyclic voltammetry (CV), electrochemical impedance spectroscopy (EIS) and differential pulse voltammetry (DPV). The CV of the proposed biosensor was processed in 10 mL of $[Fe(CN)_6]^{3-/4-}$ solution with a scan potential of −0.2 V to 0.6 V and a scan rate of 100 mV/s. EIS was carried out with a frequency range from 0.1 Hz to 100 kHz. DPV was carried out in the same solution with a potential of −0.2 V to 0.6 V, a pulse amplitude of 50 mV, a pulse width of 50 ms and a pulse period of 0.1 s. Each result would be repeated three times with the average value as the final result.

2.5. Gel electrophoresis

To verify the feasibility of the proposed biosensing strategy, 12% native polyacrylamide gel electrophoresis (PAGE) was carried out to analyze DNA products. Each lane was loaded 10 μL of samples and ran in 1 × TBE buffer at 100 V for about 80 min. Upon completion, the gel was stained by Super GelRed nuclear staining for 10 min and scanned using a Bio-Red Imaging System.

2.6. Preparation of clinical serum samples

Serums were obtained from healthy volunteers at the Southwest Hospital of Third Military Medical University with ethical approval. In brief, whole blood samples were allowed to stand at room temperature and the pale yellow supernatant was collected as serum. 10-fold diluted serums were prepared by adding 30 μL of serums into 270 μL of the competitive buffer. Afterwards, 10 pM, 1 pM, 100 fM and 10 fM miRNA-25 serum samples were obtained by adding a certain amount of miRNA-25 to the diluted serums.

3. Result and discussion

3.1. Design principle of the biosensing strategy

The principle of the DNA nanomaterial-based miRNAs detection biosensor is illustrated in Scheme 1. The approach consists of two main components: a Y-DNA probe and a non-linear hybridization chain reaction (non-linear HCR) system. Y-DNA probes were composed of two supporting sequences (Y1, Y2) and a competitive probe (Y3). Firstly, Y-DNA probes were synthesized by slow cooling and parts of Y1, Y2 and Y3 could hybridize to each other. Tactfully, a single base deficiency was designed between Y2 and Y3 to improve the efficiency of the next competitive combination. Besides, the ends of Y1, Y2 were able to initiate the subsequent non-linear HCR after exposure. After fixing Y-DNA probes on the surface of gold electrodes, miRNA-25 was introduced and could completely hybridize with Y3. Due to the unpaired domain between Y2 and Y3, the miRNA-25 were able to replace the support sequences and kept Y3 away from Y-DNA nanostructures. Therefore, the trigger ends which were protected by Y3 before were exposed and initiated non-linear HCR. This amplification system comprised two double-stranded substrates (S1, S2) and two single-strand helpers (H1, H2). The end-triggers hybridized to the exposed toehold of S1, replacing a portion of S1b. Then H1 bound to the newly exposed toehold of S1b. Since there were bridge loops in the middle of S1, S1b was released from the original double-stranded substrate and formed a new by-product B1. As a result, the S1a stand exposed two identical sequences that could serve as new triggers for interacting with the toehold of S2. The H2 stand similarly hybridized to newly exposed toeholds of S2b, removing S2b from the previous substrates. Until now, the reaction had led to the formation of a branched DNA nanostructure with two triggering toeholds, which were identical to the previous ones and could initiate a new round of reaction. A dendrimer-like DNA nanostructure would be constructed by cascade reactions, and finally the amplification of the signal could be achieved.

3.2. Feasibility of the biosensing strategy

The stepwise fabrication of the biosensor was demonstrated by the results of PAGE (Fig. S1), CV and EIS. As can be seen from Fig. 1, the bare gold electrodes exhibited a couple of reversible redox peaks of $[Fe(CN)_6]^{3-/4-}$ and a very small semicircle of EIS signal, which reflected the interfacial electrons transfer resistance (R_{et}) (curve a). These results indicated that the surface was clear enough for the next operation. When Y-DNA probes were fixed on the electrodes, the redox intensity decreased and R_{et} increased obviously (curve b). These changes were due to the fact that Y-DNA probes modified electrodes hold more negative charges. And the repulsive reaction between DNA and $[Fe(CN)_6]^{3-/4-}$ would reduce the ability of electrons transfer. The redox intensity and R_{et} continued to decrease and increase after adding MCH to the surface, since MCH could block the uncovered space of electrode (curve c). Afterwards, with the introduction of miRNA-25, the sequence of Y3 was released from electrodes, resulting in increased intensity and decreased R_{et} (curve d). Finally, non-linear HCR caused cascade amplification and produced a dramatic decrease in redox intensity and an increase in R_{et} (curve e), because the complex construction carried more negative charges on the electrode surfaces. The above results demonstrated the proposed biosensor was assembled successfully.

3.3. Optimization of the biosensing strategy

To achieve the best detecting efficiency, various experimental parameters including the concentration of Y-DNA probes and non-linear HCR components, the reaction times and temperatures of capturing target miRNA and non-linear HCR were required to be optimized. Initially, to maximize the sensitivity of the assay, different reaction times were experienced. Fig. 2a shows the effect of various reaction times for miRNAs hybridization. In order to quantify the results accurately, differential pulse voltammetry (DPV) changes were applied to evaluate the efficiency of the reaction. The signal changes increased gradually with the increase of reaction time and arrived relatively stable after 120 min, indicating that 120 min was sufficient to identify and hybridize target miRNAs. Thus, 120 min was employed as the proper reaction time for miRNAs competitive hybridization. In addition, non-linear HCR as the final signal amplification reaction would directly influence the sensitivity of the biosensing strategy. The reaction time was investigated and the results were showed in Fig. 2b. As the reaction time increased, the signal changes increased and remained constant after 3 h. So 3 h was selected to be the best reaction time for non-linear HCR. The optimization results showed that prolonging the reaction time was ineffective because the reaction would reach equilibrium after a period of time.

The concentration of Y-DNA would also influence the performance of the electrochemical biosensor. Since the concentration of too high or too low were not suitable for this study, we chose 5 nM, 10 nM, 15 nM,

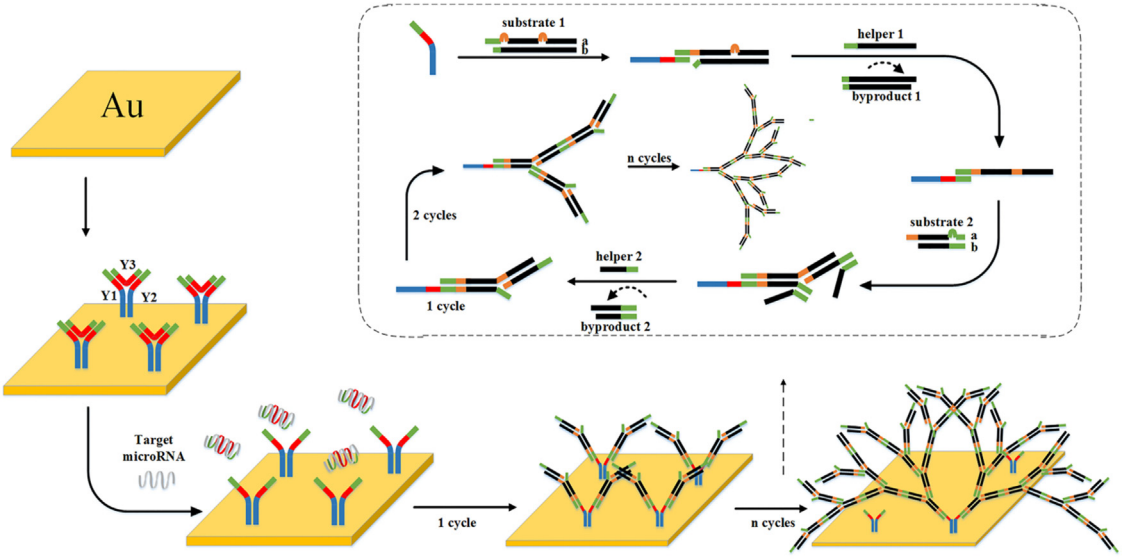

Scheme 1. Schematic illustration of the proposed biosensor for miRNAs detection.

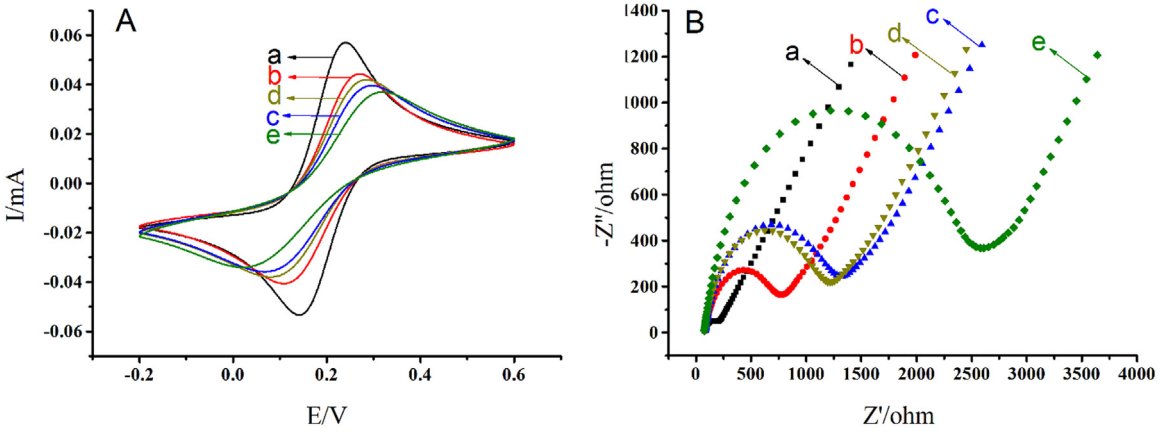

Fig. 1. CV (A) and EIS (B) characteristics of different modified electrode. (a) bare gold electrode (GE), (b) Y-DNA/GE, (c) MCH/Y-DNA/GE, (d) miRNA-25/MCH/Y-DNA/GE, (e) non-linear HCR/miRNA-25/MCH/Y-DNA/GE.

20 nM and 25 nM as the candidate concentrations. As shown in Fig. 2c, the signal changes increased with the augment of Y-DNA concentration, reached the maximum at 15 nM, and decreased slowly, indicating an optimum probe concentration of 15 nM. Similarly, the concentration of non-linear HCR components were also optimized and showed in Fig. 2d. The components of non-linear HCR contained S1, S2, H1 and H2, which dissolved in hybridization buffer at the same concentration. And this concentration was used as the optimal concentration. As the concentration increased, the signal changed gradually, reaching a maximum at 40 nM and decreasing slowly with increasing concentrations. Therefore, 40 nM was chosen as the appropriate concentration of non-linear HCR components. The experimental results indicated that excess substrates couldn't participate in the reaction, but would influence the amplification efficiency.

What's more, in order to investigate satisfying miRNAs competitive binding reaction temperature, the biosensing strategy was detected at different reaction temperatures. Since 37 ℃ is the most common temperature of physiological reaction, approximate temperatures were chosen as the experiment parameters. As depicted in Fig. 2e, with the raise of miRNAs hybridize reaction temperature, the signal changes increased, rose to a maximum value at 35 ℃, and decreased as the reaction temperatures increased. Hence, 35 ℃ was selected as the optimal miRNAs hybridize reaction temperature in this experiment. The performances of non-linear HCR performance at different temperatures were also perfected in the same way. As shown in Fig. 2f, the signal changes increased and reached the maximum at 39 ℃, then at higher temperatures, the signal changes decreased gradually. This trend indicated that the appropriate temperature for non-linear HCR was 39 ℃. In addition, there were no significant differences between the signal changes at 37 ℃ and optimum temperatures, so 37 ℃ could be used as a reaction temperature in practical applications to simply the operations.

3.4. Performance of the biosensing strategy

To further explore the quantitative accuracy of the proposed strategy, a rigorous calibration curves for the detection of miRNA-25 from the low to high concentrations was performed. Under the optimized conditions, different concentrations of miRNA-25 were analyzed by the biosensor. The signal changes of different concentrations of the target miRNA produced by this strategy are illustrated in Fig. 3. The electrochemical signal changes increased with the increment of target miRNA, and revealed a satisfying linear relationship with the logarithm of miRNA-25 concentration. The linear regression equation is $-\Delta I/I = 0.03252\lg c + 0.3121$ with the concentrations of miRNA-25 ranging from 1 fM to 10 pM. (ΔI is equal to the difference between the peak current of final results and the peak current after miRNA-25 competitive binding reaction. c is the miRNA-25 concentration, $R^2 = 0.9977$). The threshold of detection limit was set to 3-fold standard deviation

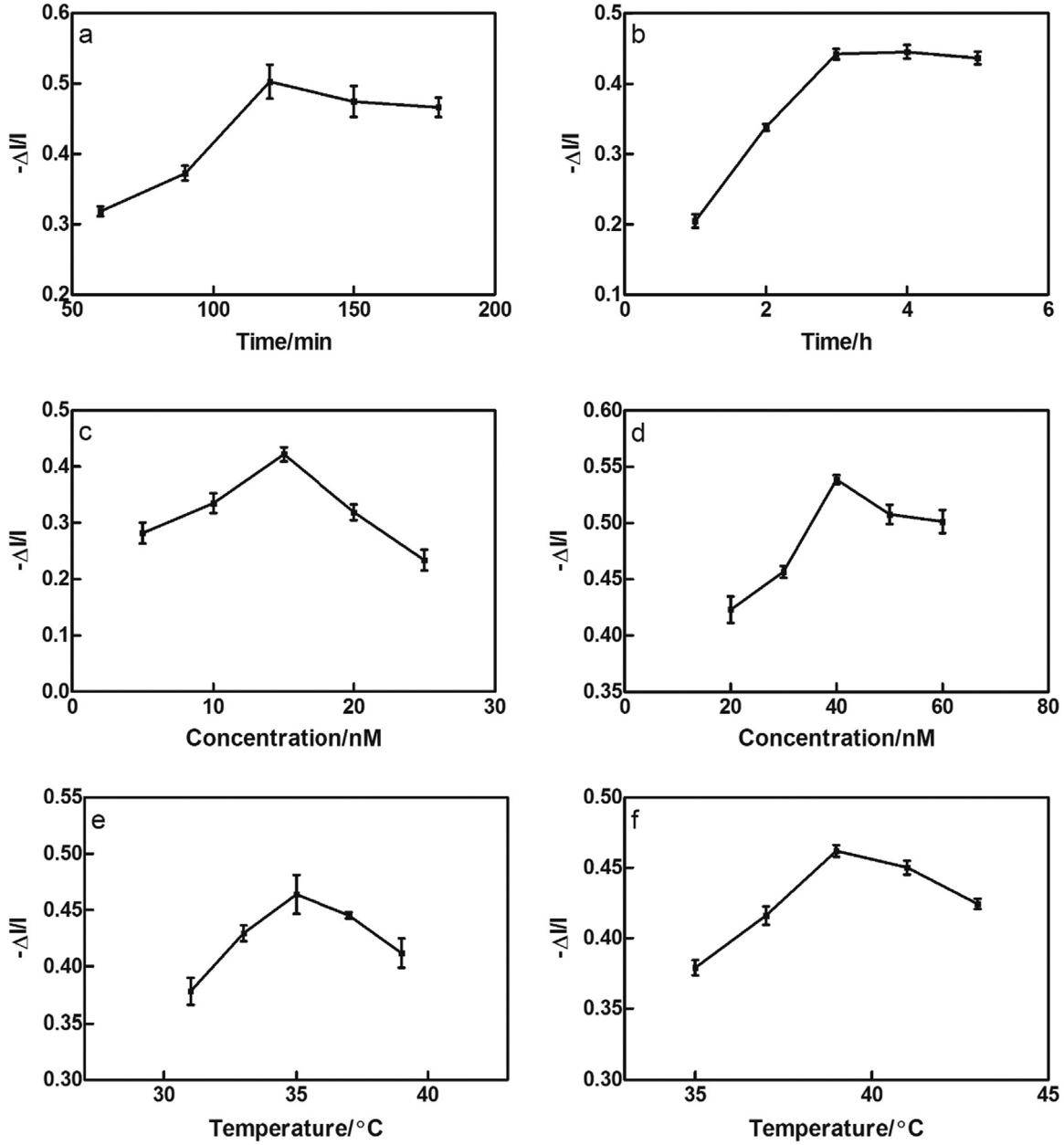

Fig. 2. Optimizations of experimental parameters: (a) reaction time of miRNA hybridization, (b) reaction time of non-linear HCR, (c) concentration of Y-DNA probes, (d) concentration of non-linear HCR components, (e) reaction temperature of miRNA hybridization, (f) reaction temperature of non-linear HCR. The electrochemical signal changes were obtained with 1 nM target miRNA.

(SD) above blank. Therefore, the detection limit was determined as 0.3334 fM. Furthermore, the analytical performance of this biosensing method was compared with other reported miRNAs detection methods (Table S2). As shown, this work exhibited an attractive lower detection limit and a relatively wider linear range than other label-free biosensors. Its detection limit can reach the level of biosensors that required labeling or other complicated modifications. The characteristic of label-free and enzyme-free is an important advantage in practical applications because it could reduce the requirements of operating circumstances and decrease cost. The linear range and low detection limit reflect the significant performance of this strategy and suggest that the proposed biosensor is desirable for detecting miRNAs in clinical assays.

3.5. Selectivity and stability of the biosensing strategy

Mutations of nucleic acids, even single base mutations, can affect the whole structures and functions of nucleic acids. Therefore, an accurate assessment of the proposed biosensor's ability to distinguish mutations is also a significant aspect of appraising its performance. For this reason, a comparison between the mutation targets and perfect complementary target was performed. As shown in Fig. 4, single-base mismatched miRNA-25, double-bases mismatched miRNA-25, three-bases mismatched miRNA-25 and three different miRNAs (miRNA-21, miRNA-107 and miRNA-145) were designed as the possible contrastive substances with target miRNA-25. The concentration of these miRNAs were 1 nM which was higher than the limit of detection to ensure the reliability of the results. And the results of target miRNA were significantly different from those of other analogs ($P < 0.001$). The results exhibits the good performance in distinguishing between perfect

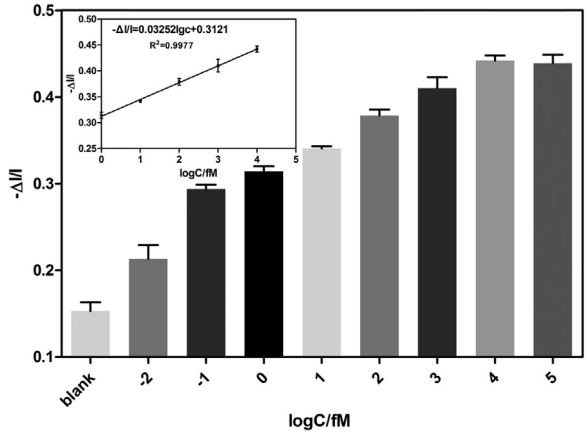

Fig. 3. Calibration curve between the electrochemical signal changes and target miRNA concentrations from 0.01 fM to 100 pM Inset shows the linear relationship between the signal changes and the logarithm of the miRNA-25 concentrations. Error bars represent the standard deviations measured from three different tests.

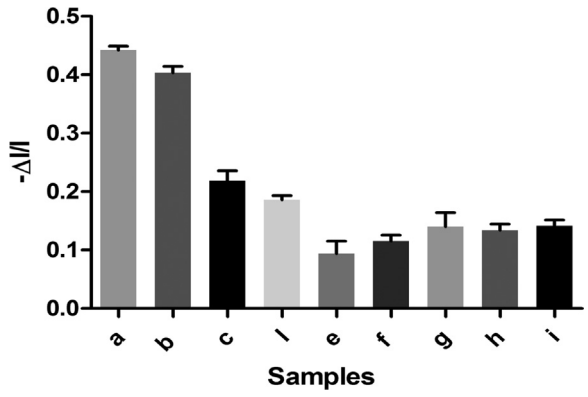

Fig. 4. Selectivity of the proposed electrochemical biosensor towards target miRNA. (a) miR-25, (b) miRNAs mixture including miR-25, miR-21, miR-107 and miR-145, (c) single-base mismatched miR-25, (d) two-bases mismatched miR-25, (e) three-bases mismatched miR-25, (f) miR-21, (g) miR-107, (h) miR-145, (i) blank. The electrochemical signal changes were obtained with 1 nM miRNAs, error bars represent the standard deviations measured from three different tests.

target sequences and mismatched target sequences, which would be potential for detecting single base mutations. Additionally, when miRNA-25 was mixed with the three different miRNAs sequences mentioned before, the signal changes were nearly the same as the value obtained from miRNA-25 only. This capacity to resist interferences is of great significance in clinical applications, since numerous disturbances exist in serum samples. Moreover, to further improve the practicability of the designed strategy, the stability of the prepared biosensor was evaluated. As shown in Fig. S2, the Y-DNA modified electrodes were stored at 4 ℃ and used to measure miRNA-25 every 7 days. After 21 days, the biosensor was still able to maintain 90.61% of the corresponding initial response, indicating the satisfactory stability of the proposed biosensor. And stability could help to extend the life of each prepared biosensor. These two characteristics would enable the biosensor to reveal satisfactory performance in clinical assays.

3.6. Analytical application of the biosensing strategy

Evaluating the performance of the proposed biosensor in serums is an essential step in confirming its usefulness for clinical assays. Various concentrations of miRNA-25 were added to the 10-fold diluted healthy human serum samples, which helped to reduce the influence of proteins. As shown in Table 1, serum samples with miRNA-25 concentrations of 10 pM, 1 pM, 100 fM and 10 fM were prepared and measured. Three samples were detected for each concentration and the signal changes were the average of three results. The measured concentrations of the samples were calculated by bring signal change values into the linear regression equation mentioned above. It could be seen that the relative standard deviation (RSD) of the contents ranged from 3.90% to 5.61% and the recovery ranged from 90% to 107.1%, indicating a good match between the measured experimental values and the genuine concentrations of the miRNA-25 in the serum samples. The results demonstrated that the biosensor was available to detect miRNA-25 in real serum samples. The satisfying performance would enable the determination of target miRNAs in clinical samples, thereby facilitating the use of miRNAs as biomarkers for early diagnosis of diseases.

Table 1
Actual and measured concentration of miR-25 in human serum samples (n = 3).

Added	Measured	RSD/%	Recovery/%
10 pM	10.71 pM	3.90	107.1
1 pM	0.90 pM	4.70	90
100 fM	97.28 fM	5.61	97.28
10 fM	10.48 fM	4.78	104.8

4. Conclusions

In summary, we have successfully developed an ultrasensitive, label-free electrochemical biosensor for rapid, sensitive and specific detecting of miRNA-25 by using Y-shaped DNA nanostructures as capture probes and non-linear hybridization chain reaction as the signal amplification method. Stable Y-DNA nanostructures serve as probes for the recognition and capture of miRNAs. Competitive binding between the target miRNA and Y-DNA resulted in disintegration of the Y-DNA structures and explosion of triggers, which could initiate subsequent reactions. This competitive binding method significantly enhances the specificity of the biosensor. Meanwhile, the non-linear HCR further amplifies electrochemical signal changes, paving a promising path for sensitive and specific detection of target miRNAs. Under optimal conditions, the biosensor responds linearly to miRNA-25 over a concentration range of 1–10,000 fM with a limit detection of 0.3334 fM. The biosensor has achieved high specificity for miRNA-25 detection compared to single base mutations and other miRNAs. What's more, the biosensor achieves a cheap and easy-to-use miRNA-25 assay in serum samples which provides a promising potential in early clinical diagnoses and treatments. Compared with other miRNAs biosensing strategies, this proposed method shows better specificity and low detection limit. In summary, this biosensing strategy may hold great potential to expand the application of DNA nanomaterials in bioassays and to come true early and effective determination of various diseases.

Acknowledgments

This work was supported by the National Natural Science Foundation of China (Grant No. 81430053, 81430054, 81401751) and the Medical Research Funding of PLA of China (No. AWS14C003-2).

Appendix A. Supporting information

Supplementary data associated with this article can be found in the online version at doi:10.1016/j.bios.2018.11.028.

References

Azzouzi, S., Mak, W.C., Kor, K., Turner, A.P.F., Ali, M.B., Beni, V., 2017. Biosens. Bioelectron. 92, 154–161.

Bi, S., Yue, S., Zhang, S., 2017. Chem. Soc. Rev. 46, 4281–4298.
Brown 3rd, C.W., Buckhout-White, S., Díaz, S.A., Melinger, J.S., Ancona, M.G., Goldman, E.R., Medintz, I.L., 2017. ACS Sens. 2, 401–410.
Chang, C.C., Chen, C.Y., Chuang, T.L., Wu, T.H., Wei, S.C., Liao, H., Lin, C.W., 2016. Biosens. Bioelectron. 78, 200–205.
Ding, X., Cheng, W., Li, Y., Wu, J., Li, X., Cheng, Q., Ding, S., 2017. Biosens. Bioelectron. 87, 345–351.
Flowers, E., Froelicher, E.S., Aouizerat, B.E., 2013. Biol. Res. Nurs. 15, 167–178.
Franklin, O., Jonsson, P., Billing, O., Lundberg, E., Öhlund, D., Nyström, H., Lundin, C., Antti, H., Sund, M., 2018. Ann. Surg. 267, 775–781.
Hausser, J., Zavolan, M., 2014. Nat. Rev. Genet. 15, 599–612.
He, Y., Yang, X., Yuan, R., Chai, Y., 2017. Anal. Chem. 89, 8538–8544.
Hu, F., Xu, J., Chen, Y., 2017. Anal. Chem. 89, 10071–10077.
Li, Y., Chang, Y., Yuan, R., Chai, Y., 2018. ACS Appl. Mater. Interfaces 10, 25213–25218.
Li, Y., Tseng, Y.D., Kwon, S.Y., D'Espaux, L., Bunch, J.S., McEuen, P.L., Luo, D., 2004. Nat. Mater. 3, 38–42.
Liu, C., Chen, C., Li, S., Dong, H., Dai, W., Xu, T., Liu, Y., Yang, F., Zhang, X., 2018. Anal. Chem. 90, 10591–10599.
Liu, G., Niu, X., Meng, X., Zhang, Z., 2018. J. Thorac. Dis. 10, 3206–3215.
Liu, S., Gong, H., Sun, X., Liu, T., Wang, L., 2015. Chem. Commun. 51, 17756–17759.
Lu, S., Wang, S., Zhao, J., Sun, J., Yang, X., 2017. Anal. Chem. 89, 8429–8436.
Lu, J., Wu, L., Hu, Y., Wang, S., Guo, Z., 2018. Biosens. Bioelectron. 109, 13–19.
Miao, P., Jiang, Y., Zhang, T., Huang, Y., Tang, Y., 2018. Chem. Commun. 54, 7366–7369.
Nehra, A., Pal Singh, K., 2015. Biosens. Bioelectron. 74, 731–743.
Niu, S., Jiang, Y., Zhang, S., 2010. Chem. Commun. 46, 3089–3091.
Papadaki, C., Stratigos, M., Markakis, G., Spiliotaki, M., Mastrostamatis, G., Nikolaou, C., Mavroudis, D., Agelaki, S., 2018. Breast Cancer Res. 20, 72.
Peng, X., Liang, W.B., Wen, Z.B., Xiong, C.Y., Zheng, Y.N., Chai, Y.Q., Yuan, R., 2018a. Anal. Chem. 90, 7474–7479.
Peng, X., Zhu, J., Wen, W., Bao, T., Zhang, X., He, H., Wang, S., 2018b. Biosens. Bioelectron. 118, 174–180.
Su, S., Wu, Y., Zhu, D., Chao, J., Liu, X., Wan, Y., Su, Y., Zuo, X., Fan, C., Wang, L., 2016. Small 12, 3794–3801.
Tian, T., Wang, J., Zhou, X., 2015. Org. Biomol. Chem. 13, 2226–2238.
Urbanek, M.O., Nawrocka, A.U., Krzyzosiak, W.J., 2015. Int. J. Mol. Sci. 16, 13259–13286.
Wahlquist, C., Jeong, D., Rojas-Muñoz, A., Kho, C., Lee, A., Mitsuyama, S., van Mil, A., Park, W.J., Sluijter, J.P., Doevendans, P.A., Hajjar, R.J., Mercola, M., 2014. Nature 508, 531–535.
Wang, K., Lei, Y., Zhong, G.X., Zheng, Y.J., Sun, Z.L., Peng, H.P., Chen, W., Liu, A.L., Chen, Y.Z., Lin, X.H., 2015. Biosens. Bioelectron. 71, 463–469.
Xu, F.X., Su, Y.L., Zhang, H., Kong, J.Y., Yu, H., Qian, B.Y., 2014. Asian Pac. J. Cancer Prev. 15, 1197–1203.
Xu, T., Song, Y., Gao, W., Wu, T., Xu, L.P., Zhang, X., Wang, S., 2018. ACS Sens. 3, 72–78.
Xuan, F., Hsing, I.M., 2014. J. Am. Chem. Soc. 136, 9810–9813.
Yates, L.A., Norbury, C.J., Gilbert, R.J., 2013. Cell 153, 516–519.
Ye, D., Zuo, X., Fan, C., 2018. Annu. Rev. Anal. Chem. 11, 171–195.
Zhang, P., Li, Z., Wang, H., Zhuo, Y., Yuan, R., Chai, Y., 2017. Nanoscale 9, 2310–2316.
Zhou, L., Morel, M., Rudiuk, S., Baigl, D., 2017. Small 13.
Zhou, J., Yu, L., Gao, X., Hu, J., Wang, J., Dai, Z., Wang, J.F., Zhang, Z., Lu, S., Huang, X., Wang, Z., Qiu, S., Wang, X., Yang, G., Sun, H., Tang, Z., Wu, Y., Zhu, H., Fan, J., 2011. J. Clin. Oncol. 29, 4781–4788.
Zhou, X., Zhao, M., Duan, X., Guo, B., Cheng, W., Ding, S., Ju, H., 2017. ACS Appl. Mater. Interfaces 9, 40087–40093.